

# Biomechanical Effect of Filled Biomaterials on Distal Thai Femur by Finite Element Analysis

Panya Aroonjarattham<sup>1,\*</sup> KittiAroonjarattham<sup>2</sup> and Maneerat Chanasakulniyom<sup>3</sup>

---

## ABSTRACT

Giant cell tumors are frequently detected at the lower end of the distal femur. Surgery is the most effective treatment for these tumors. The experience of the surgeons determines the amount of bone removal containing the giant cell tumors (excision) and what biomaterials should be used for the bone replacement; however, the strength of the reconstructed bone has been a concern. Finite elements analysis was employed in this study to analyze the direction to fill and the appropriate quantity of biomaterial, namely polymethylmethacrylate (PMMA) or hydroxyapatite (HA), which was used to replace the bone.

With PMMA replacement, increased quantities of PMMA replacement made the maximum von Mises stress nearly constant. The surgeon should fill the PMMA replacement from the lateral to the medial side to reduce the maximum von Mises stress on PMMA. With HA replacement from the lateral to the medial side, the maximum von Mises stress slightly increased when the biomaterials were added under walking conditions and were nearly stable when added under stair climbing conditions. However, HA replacement from the medial to the lateral side produced the highest maximum von Mises stress when three parts of biomaterial were added under both conditions. The surgeon should fill the HA replacement from the lateral to the medial side to minimize the maximum von Mises stress on the HA. In addition, finite elements analysis seemed to be a useful tool, combined with the surgeons' experience to validate suitable biomaterial or an appropriate procedure for better results in bone surgery.

**Keyword:** biomaterial, distal Thai femur, finite element analysis

## INTRODUCTION

Giant cell tumor (GCT) is a locally destructive tumor which usually occurs at the epiphysis of the long bone (Thomas and Skubitz, 2009; Miller *et al.*, 2010). Tumors arise in the meta-epiphysis region predominantly in the distal femur and the proximal tibia (Klenke *et al.*, 2011). There are various treatments of GCT including:

bone curettage of the tumor, bone curettage of the tumor and filling with bone grafting (Bickels *et al.*, 1999); bone curettage of the tumor and filling with biomaterials such as polymethylmethacrylate (PMMA) cement (Campanacci *et al.*, 1990; Bini *et al.*, 1995; Wada *et al.*, 2002; Kivioja *et al.*, 2008) and hydroxyapatite (HA) (Matsumine *et al.*, 2006); and primary resection followed by allograft or prosthetic reconstruction and radiation

---

<sup>1</sup> Department of Mechanical Engineering, Faculty of Engineering, Mahidol University, Nakhon Pathom 73170, Thailand.

<sup>2</sup> Department of Orthopaedic, Faculty of Medicine, Burapha University, Chon Buri 20131, Thailand.

<sup>3</sup> Department of Mechanical Engineering, Faculty of Engineering, Bangkok Thonburi University, Bangkok 10170, Thailand.

\* Corresponding author, e-mail: panya.aro@mahidol.ac.th

therapy (Blackley *et al.*, 1999; von Steyern *et al.*, 2007). The therapy normally depends on the surgeons' decisions based on their experience which determine whether to eliminate only the tumor or the tumor and some bone (Cleveland-Clinic, 2010; Intermountain-Healthcare, 2010). As a result, some patients will lose more bone than necessary and this makes the bone weaker than normal (Yanagawa *et al.*, 2009).

This study used the finite element method to analyze the direction to fill and the appropriate quantity of biomaterial with which to fill the distal femur after the removal of bone tumor. The results from this study can be used together with the decision of the surgeons to produce the best result in benign bone tumor therapy.

## MATERIALS AND METHODS

### Three-dimensional model

A three-dimensional model of the Thai femur, knee joint and tibia was created from computerized tomography (CT) data (GE LightSpeed VCT; Chonburi, Thailand). The data were converted to two-dimensional images to construct three-dimensional models using the ITK-SNAP software (Version 2.4.0; 2012; <http://www.itksnap.org/pmwiki/pmwiki.php?n=Downloads.SNAP2>). The CT dataset was imported and allowed extended visualization and segmentation functions based on image density thresholding. To optimize the geometry of cortical surfaces, two thresholding values were applied to separate a lower thresholding and a higher thresholding value to extract the inner and outer cortical surface. The model of the Thai femur, knee joint and proximal tibia are shown in Figure 1.

The parameters of the model in use were ascertained to not exceed those of Thai femoral morphometric data (Mahaisavariya *et al.*, 2002). Therefore, this model was used to represent the Thai femur in the analysis.



**Figure 1** Three dimensional model of femur, knee joint and proximal tibia (anterior view).

### Ligament and meniscus model

The three-dimensional models of the ligament and meniscus were created using the SolidWorks CAD software (Version 2010; Mahidol University; Nakhon Pathom, Thailand) because the CT scanner did not detect the ligament and meniscus. The meniscus was created between the femur and tibia based on the shape from actual anatomy and all ligaments were created using a curve from the distal femur to the proximal tibia based on anatomical position and shape. The knee joint contains four major ligaments being the anterior cruciate ligament, posterior cruciate ligament, medial collateral ligament and lateral collateral ligament as shown in Figure 2.

### Locking plate and locking screws model

HA replacement uses the locking plate and locking screw to share the load bearing. The locking plate was scanned using the CT scanner and was converted to a three-dimensional model as shown in Figure 3. To reduce the calculation time, the model ignored the thread depth in the locking screws because the overall diameter had a greater effect.

### Virtual simulation technique

A virtual simulation technique was used to insert the model using the characteristics of actual surgery for the finite element analysis. The purpose of this study was to analyze appropriate biomaterial replacement for the patient in the operation to remove a giant cell tumor at the lower end of the femoral bone. Therefore, the model of the distal femur was divided into four parts as shown in Figure 4 to simulate the effect of the biomaterial quantities on the bone.

This study used different biomaterials replacement consisting of polymethylmethacrylate (PMMA) and hydroxyapatite (HA) reinforcement with locking plates and locking screws. The model of the femur with locking plate and tibia is shown in Figure 5.

### Finite element model

Finite element models were developed and analyzed using the MSC.MARC software

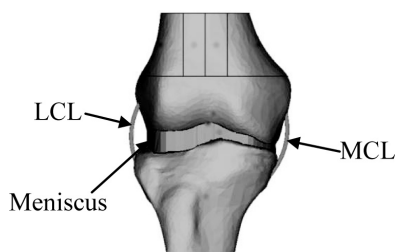


**Figure 2** Three dimensional model of Thai femoral bone and knee joint with ligament and meniscus model (LCL = Lateral collateral ligament; MCL = Medial collateral ligament).

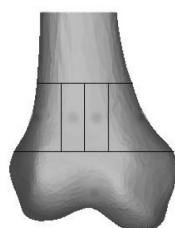


**Figure 4** Four parts of distal femur.

packages (Version 2010; Mahidol University; Nakhon Pathom, Thailand). The four-node tetrahedral elements were used to form a mesh of cortical and cancellous bone as shown in Figure 6. The four-node tetrahedral element can be used to easily mesh any type and shape of object regardless of the complexity. The finite element models for PMMA replacement had 130,529 nodes and 529,401 elements and the HA replacement reinforcement with locking plates and locking screws had 198,524 nodes and 815,368 elements.

The contact condition is used to determine the correspondence among the MSC fragments. The program aims to define the relationship of the contact using three characteristics—no



**Figure 3** Three dimensional models of locking plate and locking screws.



**Figure 5** Bone model with locking plate and locking screws.

contact, touch contact and glue contact (Paul *et al.*, 2006). The glue contact condition was applied in the current research, where the end of ligament contacts the bone. The glue contact was assumed to replace a rigidly fixed ligament on the distal femur and proximal tibia. The touch contact condition was applied in this research, where the distal femur contacts the meniscus, where the proximal tibia contacts the meniscus and where the meniscus contacts ligaments.



**Figure 6** Finite element analysis model.

### Material properties

All materials involved in the model were assumed to have linear, elastic and isotropic properties. The distal femoral bone models were replaced with the biomaterials PMMA and HA. The locking plate with locking screws was made from stainless steel (AISI 316L). The material properties, which were used for the analysis of all models, are specified in Table 1.

### Boundary conditions

The boundary conditions in this analysis represent the loads imposed on the structures and were based on daily activities such as walking and stair climbing (Heller *et al.*, 2004). Load actions on the proximal femur of all models are shown in Tables 2 and 3 for walking and stair climbing conditions, respectively, and the position of the acting force is shown in Figure 7.

## RESULTS

All results of the finite element analysis were analyzed for the equivalent total strain distribution on the distal femur and the maximum von Mises stress on the biomaterials using eight different models under walking and stair climbing conditions. The distal femur models divided the

**Table 1** Material properties assigned for finite element model (Asavamongkolkul *et al.*, 2003; Lee, 2005; Perez *et al.*, 2008; Massachusetts Institute of Technology, 2010).

Model	Young's Modulus (MPa)	Poisson's Ratio
Cortical bone	14,000	0.30
Cancellous bone	600	0.20
Meniscus	12	0.45
ACL,PCL,LCL	345	0.40
MCL	332.2	0.40
Polymethylmethacrylate	1,800	0.35
Hydroxyapatite	40,000	0.27
Stainless steel AISI 316L	200,000	0.30

ACL = Anterior cruciate ligament; PCL = Posterior cruciate ligament; MCL = Medial collateral ligament; LCL = Lateral collateral ligament

**Table 2** Load action under walking conditions (Heller *et al.*, 2004).

Position	Force (N)			Acted point
	F <sub>x</sub>	F <sub>y</sub>	F <sub>z</sub>	
Hip contact	-54.0	-32.8	-229.2	P0
Intersegmental resultant	-8.1	-12.8	-78.2	P0
Abductor	58.0	4.3	86.5	P1
Tensor fascis latae, proximal part	7.2	11.6	13.2	P1
Tensor fascis latae, distal part	-0.5	-0.7	-19.0	P1
Vastus lateralis	-0.9	18.5	-92.9	P2

F<sub>x</sub> = Force act in x-axis; F<sub>y</sub> = Force act in y-axis; F<sub>z</sub> = Force act in z-axis; P0 = Position on femoral head, which contacts pelvis; P1 = Position on proximal femur under greater trochanter on lateral side; P2 = Position on femoral shaft under lesser trochanter on lateral side; P3 = Position on femoral shaft under lesser trochanter on medial side.

**Table 3** Load action under stair climbing conditions (Heller *et al.*, 2004).

Position	Force (N)			Acted point
	F <sub>x</sub>	F <sub>y</sub>	F <sub>z</sub>	
Hip contact	-59.3	-60.6	-236.3	P0
Intersegmental resultant	-13.0	-28.0	-70.1	P0
Abductor	70.1	28.8	84.9	P1
Tensor fascis latae, proximal part	3.1	4.9	2.9	P1
Tensor fascis latae, distal part	-0.2	-0.3	-6.5	P1
Vastus lateralis	-2.2	22.4	-135.1	P2
Vastus medialis	-8.8	39.6	-267.1	P3
Ilio-tibial tract, proximal part	10.5	3.0	12.8	P1
Ilio-tibial tract, distalproximal part	-0.5	-0.8	-16.8	P1

F<sub>x</sub> = Force act in x-axis; F<sub>y</sub> = Force act in y-axis; F<sub>z</sub> = Force act in z-axis; P0 = Position on femoral head, which contacts pelvis; P1 = Position on proximal femur under greater trochanter on lateral side; P2 = Position on femoral shaft under lesser trochanter on lateral side; P3 = Position on femoral shaft under lesser trochanter on medial side.

**Table 4** Biomaterial replacement parts in distal femur models (see Table 4 for case descriptions).

Case	Number of parts with replaced biomaterial	Cortex with replaced biomaterial
A	1	Lateral side
B	2	Lateral side
C	3	Lateral side
D	4	Lateral side
E	1	Medial side
F	2	Medial side
G	3	Medial side
H	4	Medial side

cancellous bone into four parts and this bone was replaced with biomaterials from the lateral side to the medial side (cases A–D) and from the medial side to the lateral side (cases E–H) as shown in Figure 8 and Table 4. In cases A–D, the cortical

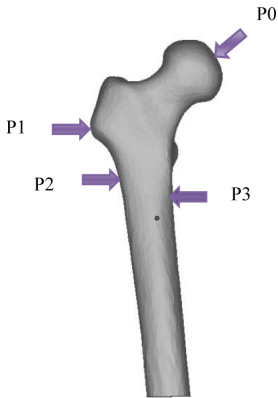


**Figure 7** Load positions on proximal femur (P0 = Position on femoral head, which contacts pelvis; P1 = Position on proximal femur under greater trochanter on lateral side; P2 = Position on femoral shaft under lesser trochanter on lateral side; P3 = Position on femoral shaft under lesser trochanter on medial side.).

bone on the lateral side was replaced with the biomaterial, but in cases E–H, the cortical bone was replaced with the biomaterial on the medial side.

**Model of equivalent total strain distribution on shaft of femoral bone**

The model of the equivalent total strain distribution on the shaft of the femoral bone after replacement with PMMA and HA under walking and stair climbing conditions is shown in Figures 9–12, respectively.

The models of the equivalent total strain distribution on the bone shaft with PMMA replacement showed the same trend as for the HA replacement. The types and quantities of biomaterials did not affect the total strain distribution on the shaft of the femoral bone. The total strain distribution on the model of both biomaterial replacements regardless of conditions did not exceed 25,000 microstrains (the maximum strain which does not lead to bone fracture according to Frost, 2003).

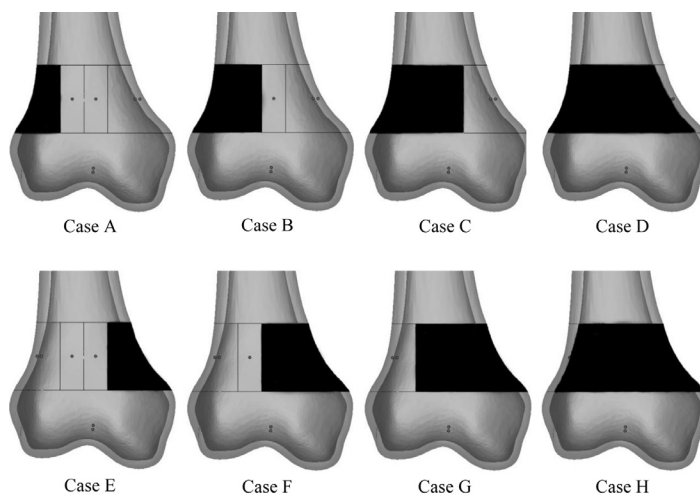


**Figure 8** Distal femoral bone models showing replacement area (black) with biomaterials from the lateral side case A to the medial case D and the medial side case E to the lateral side case H (see Table 4 for case descriptions).

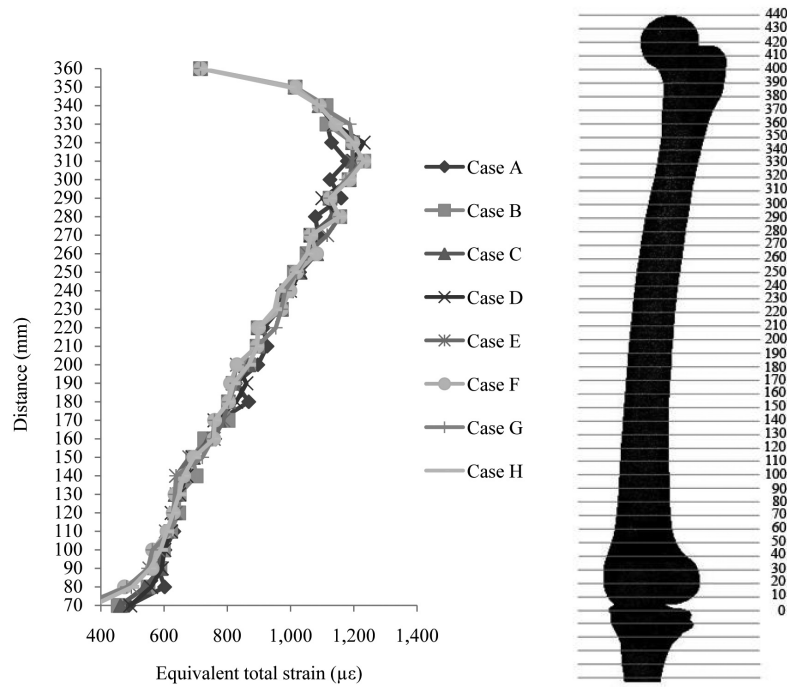


**Figure 9** Equivalent total strain distribution on shaft of femoral bone model after replacement with polymethylmethacrylate under walking conditions (see Table 4 for case descriptions).

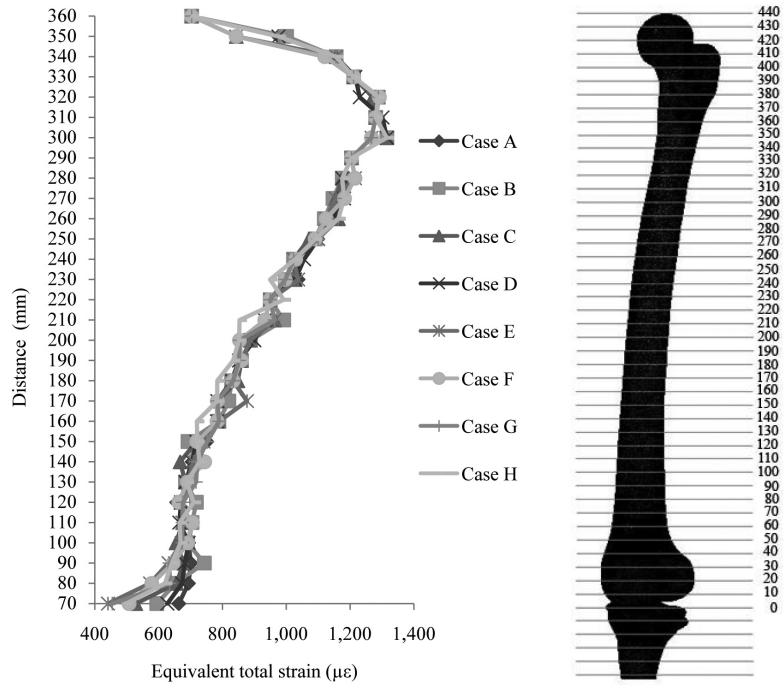


**Figure 10** Equivalent total strain on shaft of femoral bone models after replacement with polymethylmethacrylate under stair climbing conditions (see Table 4 for case descriptions).

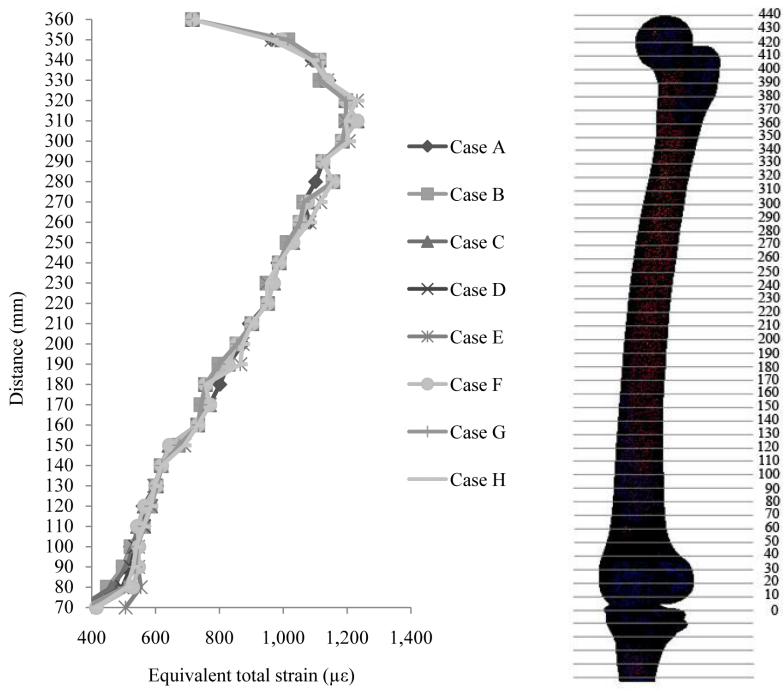


**Figure 11** Equivalent total strain on shaft of femoral bone models after replacement with hydroxyapatite under walking conditions (see Table 4 for case descriptions).

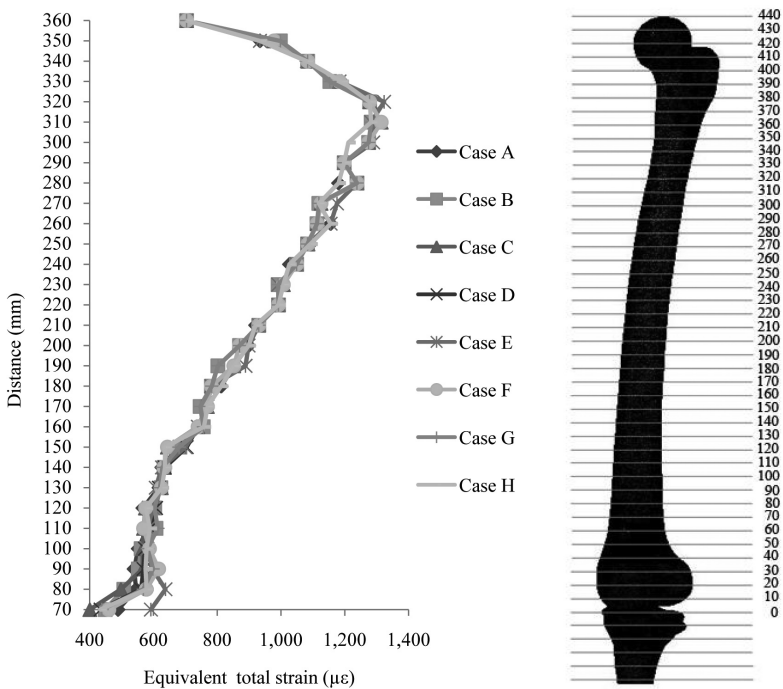


**Figure 12** Equivalent total strain on shaft of femoral bone models after replacement with hydroxyapatite under stair climbing conditions (see Table 4 for case descriptions).

### Maximum von Mises stress on polymethylmethacrylate replacement

The maximum von Mises stress levels on the PMMA replacement under walking and stair climbing conditions are shown in Figures 13 and 14.

The bone replacement from the lateral to the medial side had less maximum von Mises stress on the PMMA under both conditions than replacement from the medial to the lateral side because the body weight compressed the PMMA

on the medial side as shown in Figure 15. The PMMA in cases E–H, involving replacement of the cortex with PMMA, received a higher load on the medial side.

### Maximum von Mises stress on hydroxyapatite replacement

The maximum von Mises stress levels on the HA under walking and stair climbing conditions are shown in Figures 16 and 17.

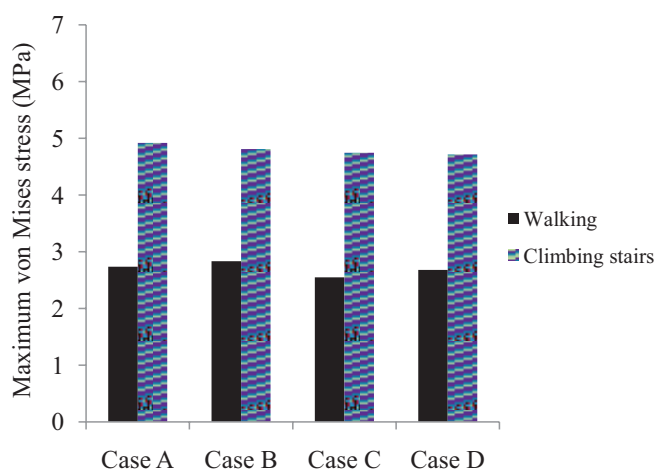


**Figure 13** Maximum von Mises stress on polymethylmethacrylate in cases A to D (see Table 4 for case descriptions).

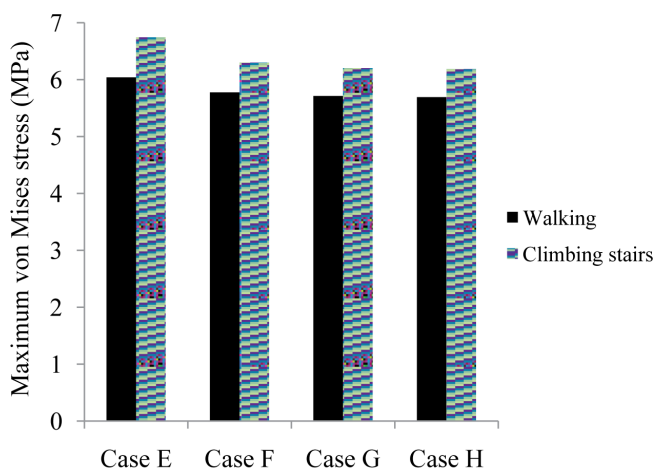


**Figure 14** Maximum von Mises stress on polymethylmethacrylate in cases E to H (see Table 4 for case descriptions).

In cases A–D, the maximum von Mises stress occurred as the amount of HA increased under both conditions. In cases E–H, the highest maximum von Mises stress occurred with HA at three parts biomaterial replacement in case G under both conditions.

All cases involving HA replacement had a higher maximum von Mises stress than all

cases involving PMMA replacement because the structure of the HA replacement was weaker than with PMMA. When the body weight load acted on the femoral head and transferred from the proximal to the distal part through the HA, the locking plates and locking screws shared the load from the bone to protect failure of the HA replacement.

**DISCUSSION**

Many authors recommend that after curettage of benign bone tumors, the defect should be filled with bone grafts or substitutes such as cement, hydroxyapatite or tricalcium phosphate (Asavamongkolkul *et al.*, 2003).

**Polymethylmethacrylate replacement**

The equivalent total strain distribution on the femoral bone was similar in all 16 cases of PMMA replacement and did not affect the bone fracture, which had a range of 337–1,231 microstrains under walking conditions and 441–1,315 microstrains under stair climbing conditions. The von Mises stress distribution on the PMMA is shown in Figures 18 and 19 under walking and stair climbing conditions, respectively.

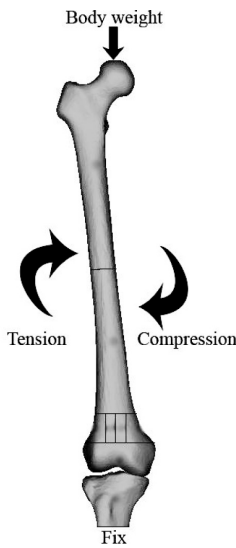


**Figure 15** Load action at medial and lateral side of femur.

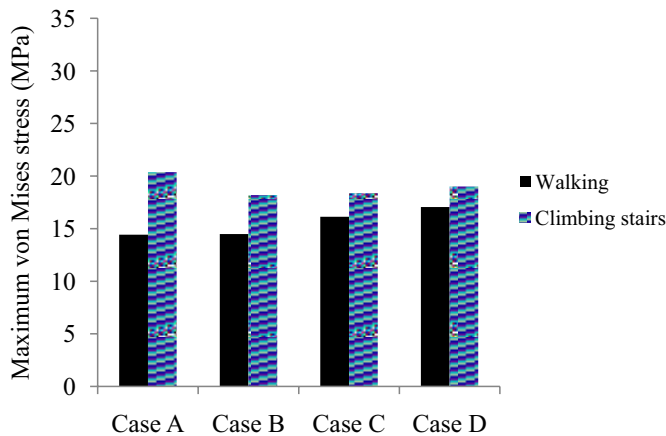


**Figure 16** Maximum von Mises stress on hydroxyapatite in cases A to D (see Table 4 for case descriptions).

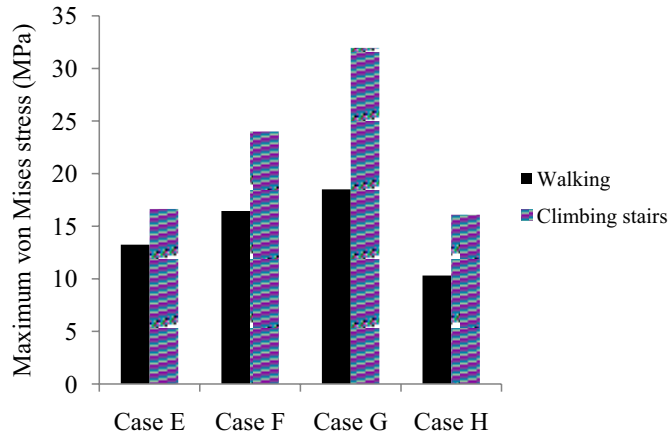


**Figure 17** Maximum von Mises stress on hydroxyapatite in cases E to G (see Table 4 for case descriptions).

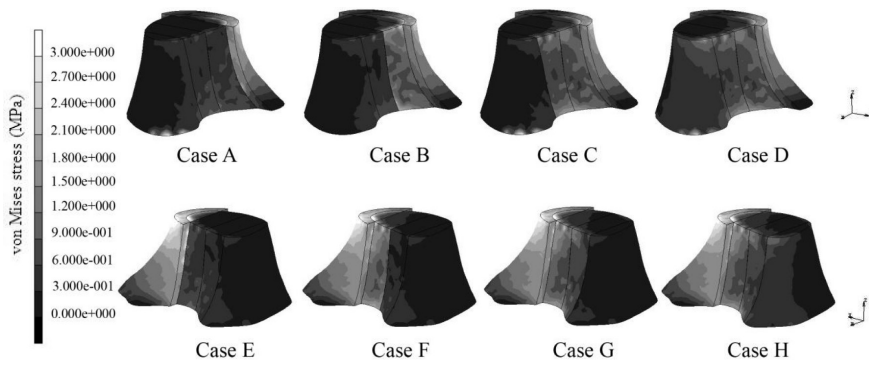


**Figure 18** von Mises stress distribution on polymethylmethacrylate replacement under walking conditions (see Table 4 for case descriptions).

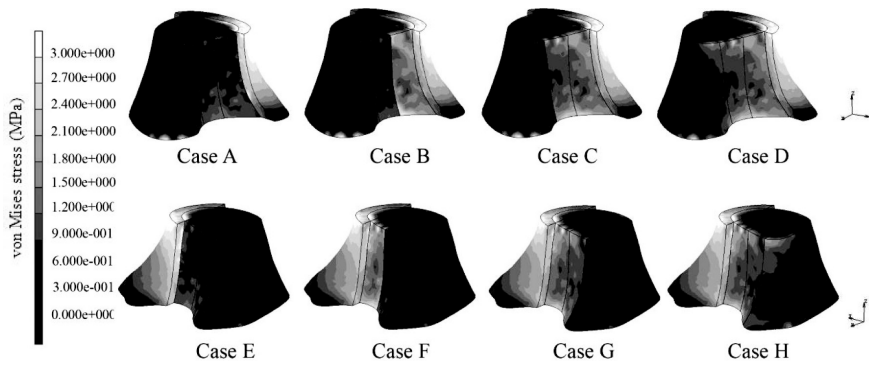


**Figure 19** The von Mises stress distribution on polymethylmethacrylate replacement under stair climbing conditions (see Table 4 for case descriptions).

The highest maximum von Mises stress on PMMA did not exceed 76 MPa, which was the yield strength of PMMA (Delft University of Technology, 2012) and the increased quantities of PMMA replacement resulted in near constant maximum von Mises stress. The surgeon should fill the PMMA replacement from the lateral to the medial side, which produced lower maximum von Mises stress than replacement from the medial to the lateral side under both conditions.

**Hydroxyapatite replacement**

The equivalent total strain distribution on the femoral bone was similar in all 16 cases of HA replacement and did not affect the bone fracture,

which had a range of 360–1,230 microstrains under walking conditions and 432–1,313 microstrains under stair climbing conditions. The von Mises stress distribution on the HA is shown in Figures 20 and 21 under walking and stair climbing conditions, respectively.

The maximum von Mises stress occurring on the HA was higher than its counterpart on the PMMA replacement but the HA replacement had the locking plate and locking screw to share the load from the biomaterial and patients should not put their full weight on the bone during the healing process. With HA replacement from the lateral to the medial side, the maximum von Mises stress slightly increased when the biomaterials

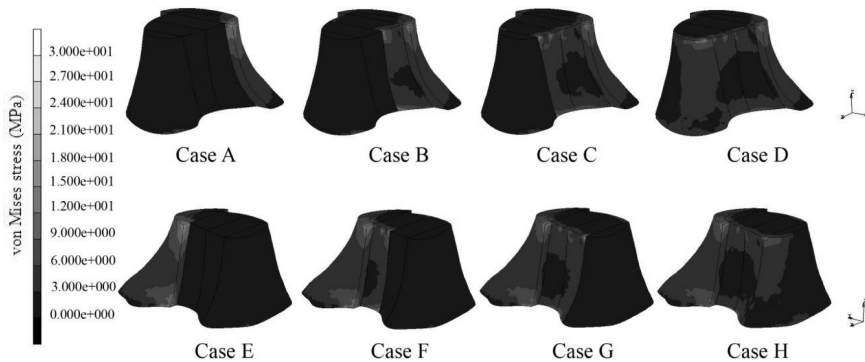


**Figure 20** von Mises stress distribution on hydroxyapatite replacement under walking conditions (see Table 4 for case descriptions).

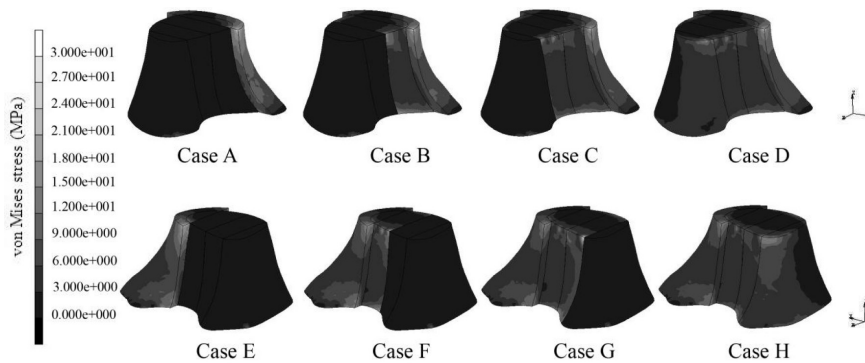


**Figure 21** von Mises stress distribution on hydroxyapatite replacement under stair climbing conditions (see Table 4 for case descriptions).

were added under walking conditions and was nearly stable when the biomaterials were added under stair climbing conditions but with HA replacement from the medial to the lateral side the highest maximum von Mises stress resulted when three part of biomaterials were added under both conditions. The HA, which replaced cortex on the medial side made the cortex weaker and the locking plate set up on the lateral side could not share the compression load on the medial side. The surgeon should fill the HA replacement from the lateral to the medial side, which had lower maximum von Mises stress than replacement from the medial to the lateral side under both conditions.

### CONCLUSION

The quantity of PMMA and HA did not affect the strain distribution on the femoral bone. Patients, treated with PMMA reconstruction could undertake rapid movement and weight bearing activity because the biomaterial could hold the load from the bone, which provided for immediate stability and the surgeon should fill the PMMA replacement from the lateral to the medial side to minimize von Mises stress on the PMMA replacement. Those treated with bone grafting procedures or HA reconstruction, who were kept in a no-weight-bearing condition using a brace or cast for 6–8 weeks followed by a radiograph, showed increased bone graft incorporation (Klenke *et al.*, 2011); thus, the surgeon should fill the HA replacement from the lateral to the medial side to minimize von Mises stress on the HA replacement.

### ACKNOWLEDGEMENT

The authors wish to thank the Faculty of Medicine, Burapha University, Thailand for their support with facilities.

### LITERATURE CITED

- Asavamongkolkul, A., A. Pongkunakorn and T. Harnroongroj. 2003. Stability of subchondral bone defect reconstruction at distal femur: comparison between polymethylmethacrylate alone and Steinmann pin reinforcement of polymethylmethacrylate. **J. Med. Assoc. Thai.** 86(7): 626–33.
- Bickels, J., I. Meller, B.M. Shmookler and M.M. Malawer. 1999. The role and biology of cryosurgery in the treatment of bone tumors. **Acta Orthop. Scand.** 70(3): 308–315.
- Bini, S.A., K. Gill and J.O. Johnston. 1995. Giant cell tumor of bone. Curettage and cement reconstruction. **Clin. Orthop. Relat. Res.** (321): 245–250.
- Blackley, H.R., J.S. Wunder, A.M. Davis, L.M. White, R. Kandel and R.S. Bell. 1999. Treatment of giant-cell tumors of long bones with curettage and bone-grafting. **J. Bone Joint Surg. Am.** 81A(6): 811–820.
- Campanacci, M., R. Capanna, N. Fabbri and G. Bettelli. 1990. Curettage of giant cell tumor of bone. Reconstruction with subchondral grafts and cement. **Chir. Organi. Mov.** 75 (1 Suppl.): 212–213.
- Cleveland-Clinic. 2010. **Benign Bone Tumors: Surgical Treatments.** 2010. [Available from: [http://my.clevelandclinic.org/disorders/benign\\_bone\\_tumors/or\\_overview.aspx](http://my.clevelandclinic.org/disorders/benign_bone_tumors/or_overview.aspx)]. [Sourced: 21 February 2012].
- Delft University of Technology. PMMA Properties. 2011. [Available from [http://www.io.tudelft.nl/research/dfs/idemat/Onl\\_db/Id123p.htm](http://www.io.tudelft.nl/research/dfs/idemat/Onl_db/Id123p.htm)]. [Sourced: 9 April 2012].
- Frost, H.M. 2003. A 2003 Update of bone physiology and Wolff's law for clinicians. **Angle Orthodontis** 74: 3–15.
- Heller, M.O., G. Bergman, J.P. Kassi, L. Claes, N.P. Hass and G.N. Duda. 2004. Determination of muscle loading at the hip joint for use in pre-clinical testing. **J. Biomech.** 38: 1155–1163.

- Intermountain-Healthcare. 2010. **Definitions of Medical Specialties: Orthopedic Surgery**. [Available from: <http://intermountainhealthcare.org/providers/specialties.html>]. [Sourced: 21 February 2012].
- Kivioja, A.H., C. Blomqvist, K. Hietaniemi, C. Trovi, A. Walloe, H.C. Bauer, P.H. Jorqensen, P. Berqh and G. Folleras. 2008. Cement is recommended in intralesional surgery of giant cell tumors: a Scandinavian Sarcoma Group study of 294 patients followed for a median time of 5 years. **Acta Orthop.** 79(1): 86–93.
- Klenke, F.M., D.E. Wenger, C.Y. Inwards, P.S. Rose and F.H. Sim. 2011. Giant cell tumor of bone: Risk factors for recurrence. **Clin. Orthop. Relat. Res.** 469: 591–599.
- Lee, C. 2005. Properties of bone cement: The mechanical properties of PMMA bone cement, pp. 60–66. *In* S. Breusch and H. Malchau, (eds.). **The Well-Cemented Total Hip Arthroplasty**. 1st ed. Springer Verlag. Berlin, Germany.
- Mahaisavariya, B., K. Sitthiseripratip, T. Tongdee, E.L.J. Bohez, J.V. Sloten and P. Oris. 2002. Morphological study of the proximal femur: a new method of geometrical assessment using 3-dimensional reverse engineering. **Med. Eng. Phy.** 24: 617–622.
- Matsumine, A., K. Katsuyuki, T. Matsubara, A. Okamura, N. Okuyama, S. Miyazaki, K. Shintani and A. Uchida. 2006. Calcium phosphate cement in musculoskeletal tumor surgery. **J. Surg. Oncol.** 93: 212–220.
- Miller, I.J., A. Blank, S.M. Yin, A. Mcnickle, R. Gray and S. Gitelis. 2010. A case of recurrent giant cell tumor of bone with malignant transformation and benign pulmonary metastases. **Diagn. Pathol.** 5(62): 1–7.
- Parez, A., A. Mahar, C. Negus, P. Newton and T.J. Impellous. 2008. A computational evaluation of the effect of intramedullary nail material properties on the stabilization of simulated femoral shaft fracture. **Med. Eng. Phy.** 30: 755–760.
- Paul, Z., B. David, E.G. Allan and P. Marcello. 2006. Notching of the anterior femoral cortex during total knee arthroplasty. **J. Arthroplasty** 21: 737–743.
- Massachusetts Institute of Technology. 2010. **Material Property Database: PMMA**. [Available from: <http://www.mit.edu/~6.777/matprops/pmma.htm>]. [Sourced: 11 November 2010].
- Thomas, D.M. and K.M. Skubitz. 2009. Giant cell tumour of bone. **Curr. Opin. Oncol.** 21(4): 338–344.
- von Steyern, F.V., I. Kristiansson, K. Jonsson, P. Mannfolk, D. Heinegard and A. Rydholm. 2007. Giant cell tumour of the knee: The condition of the cartilage after treatment by curattage and cementing. **J. Bone Joint Surg. (Br)**. 89-B(3): 361–365.
- Yanagawa, T., H. Watanabe, T. Shinozaki and K. Takagishi. 2009. Curettage of benign bone tumors without grafts gives sufficient bone strength. **Acta Orthopaedica.** 80(1): 9–13.
- Wada, T., M. Kaya, S. Nagoya, S. Kawaquchi, K. Isu, T. Yamashita, S. Yamawaki and S. Ishii. 2002. Complications associated with bone cementing for the treatment of giant cell tumors of bone. **J. Orthop. Sci.** 7(2): 194–198.